This document is downloaded from DR‑NTU (https://dr.ntu.edu.sg)
Nanyang Technological University, Singapore.

Effect of carbon nanotubes and their dispersion on electroless Ni–P under bump metallization for lead‑free solder interconnection

Hu, Xiao; Yang, Ying; Chen, Zhong; Chan, Yan Cheong; Xu, Sha

2014

Xu, S., Hu, X., Yang, Y., Chen, Z., & Chan, Y. C. (2014). Effect of carbon nanotubes and their dispersion on electroless Ni–P under bump metallization for lead‑free solder interconnection. Journal of materials science : materials in electronics, 25(6), 2682‑2691.

https://hdl.handle.net/10356/102893

https://doi.org/10.1007/s10854‑014‑1929‑8

© 2014 Springer Science+Business Media New York. This is the author created version of a work that has been peer reviewed and accepted for publication by Journal of materials science : materials in electronics, Springer Science+Business Media New York. It incorporates referee’s comments but changes resulting from the publishing process, such as copyediting, structural formatting, may not be reflected in this document. The published version is available at: [http://dx.doi.org/10.1007/s10854-014-1929-8].

Downloaded on 25 Aug 2022 18:41:33 SGT

Effect of carbon nanotubes and their dispersion on electroless Ni-P under bump metallization for lead-free solder interconnection

Sha Xu[a], Xiao Hu[a], Ying Yang[b], Zhong Chen[b], Yan Cheong Chan[a,*],

[a]Department of Electronic Engineering, City University of Hong Kong,

Tat Chee Avenue, Kowloon Tong, Hong Kong

[b]School of Materials Science and Engineering, Nanyang Technological University,

Singapore 639798, Singapore

*Corresponding author: eeycchan@cityu.edu.hk

Abstract

Electroless Ni-P under bump metallization (UBM) has advantages of even surface, low cost and simplicity to deposit, but their mechanical strength, corrosion resistance and stability still face challenges under high soldering temperature. Incorporating carbon nanotubes (CNTs) into electroless Ni-P UBM might be expected to provide Ni-P-CNT composites with high mechanical strength and stability. Ni-P-CNT composite coatings as well as Ni-P coatings were fabricated by electroless plating process. In order to homogeneously disperse CNTs in composite coatings, acid pre-treatment and surfactant dispersant were introduced. During composite electroless plating, the ultrasonic agitation was also employed. In this study, Scanning electronic microscopy (SEM) was used to observe the morphology and the CNTs were proved to be uniformly distributed in Ni-P-CNT coatings by SEM and atomic force microscopy (AFM). It was verified that the surface of the composite was quite smooth and continuous; CNTs are equably embedded in the matrix, which is advantageous for conductivity, mechanical strength and corrosion resistance. Shear tests were conducted to evaluate the effect of CNT reinforcement

on the mechanical properties of joints, and the joints with CNT additions exhibited higher shear strength at different reflow cycles. Moreover, deposition mechanism of CNTs with Ni was analyzed and confirmed by Transmission Electron Microscopy (TEM). Factors that affecting plating process was also discussed, and the optimum plating condition was suggested in this study.

Key words: under bump metallization; electroless deposition; Carbon nanotube; Ni-P.

1, Introduction

In the electronic industry, solder interconnections play a crucial role to provide necessary electrical, mechanical and thermal continuity at various levels of assembly. As high-density packaging requires fine pitches and tiny sizes, the conventional solder interconnection technology cannot guarantee satisfactory mechanical strength even using the same alloy material or under the same service condition. Thus, the mechanical integrity and other properties of miniaturized interconnection are crucial reliability issues [1]. Moreover, with the implementation of Waste Electrical and Electronic Equipment (WEEE) and Restriction of the Use of Hazardous Substances in Electrical and Electronic Equipment (RoHS Directive), lead-free solder alloys are replacing the traditional SnPb alloys which have been successfully employed in electronic industry for decades. However, many new interconnects reliability issues especially the mechanical degradation, arise along with the application of lead-free solders, due to their high reaction temperature and high dissolution rate [2,3]. Because the lead-free alloy systems normally have higher melting temperature and longer peak temperature time (time above melting point), it may not only expose the IC components to the challenge of overheating, but also lead

to rapid and excessive growth of intermetallic compounds (IMC), which are brittle and porous [4]. This mechanical degradation would hence result in deleterious effect on the solder joint reliability if no proper enhancement was made.

A great deal of experiments on improving the reliability of the lead-free solder interconnects have been performed, and one of the most effective and economically affordable approach is to incorporate appropriate foreign particles, such as metallic, ceramic particles, into the solder alloy [5]. These foreign particles normally act as reinforcement phase. Gao et al. studied the enhanced creep resistance of a Sn-3.5Ag solders by introducing micro-sized Ag, Ni, or Cu particles, and found that solder joints reinforced with Ni particles were about 30 times more creep resistant than plain Sn-3.5Ag solder joints [6,7]. Shen et al. studied eutectic Sn-9Zn solder alloys with nano-sized ZrO_2 particles and significantly improved their hardness as well as shear strength [8]. A.K. Gain et al. studied the microstructure, thermal property and hardness of Sn-3.5Ag-0.25Cu solders containing 1 wt.% TiO_2 nanoparticles, and showed that after the addition of nano-TiO_2, the solder alloys had finer microstructure and higher hardness than plain Sn-3.5Ag-0.25Cu solders at all numbers of reflow cycles [9]. These previous work are very meaningful and effective to enhance the mechanical properties of solder joints, however, most of them focused on reinforcing solder alloys, while little attention has been paid to under bump metallization (UBM), which is also correlated to many failure modes. In reality, to form good metallurgical bond during soldering reaction, UBM material is equally important with solder alloy material. In this study, a novel method of fabricating enhanced UBM was proposed to improve mechanical integrity of solder interconnects.

Nowadays, electroless Ni-P is the most widely used UBM material, and it acts as a diffusion barrier film on the pad finish for flip-chip and BGA solder bumps. Although Ni-P electroless

plating has advantages of even surface, low cost and simplicity to deposit, the mechanical strength and stability of the barrier film still faces challenge under high soldering reaction temperature. Similarly, incorporating reinforcement phase into electroless Ni–P, known as electroless composite coatings, was considered as an promising approach to improve the properties of Ni-P UBM [10,11]. And it is reported by some researchers that foreign particles can form better bond with UBM material [12,13]. The conventional electroless composite coatings are implemented by adding micro-sized particles, such as SiC, Si_3N_4, BN, PTFE, diamond, graphite, Al_2O_3 to electroless plating bath. With the evolution of modern electronic industry, micro-sized composite coatings cannot meet the needs of nowadays, and nano-scaled reinforcement particles come in age owing to their excellent performances. Among all the nano-sized candidates, CNTs have received much attention due to their high mechanical strength, Young's modulus, low density and superb chemical stability [14-17]. Moreover, CNTs are low mass-density material, which can be loaded into almost any host matrix of polymer, metal and ceramic without increasing original weight. They are considered as promising filler material to break through the performance limits of other various materials. Yang et al. successfully fabricated electroless Ni-P-CNT composite coatings, and found CNTs can significantly improve the electrochemical characteristics of composite coatings and enhance their corrosion resistance [18]. Zarebidaki et al. also reported that CNTs can improve both corrosion resistance and micro hardness of pristine electroless Ni-P layer [19]. However, there are little work studied the deposition mechanism and the dispersion of CNTs, which is a key factor for homogeneous CNT distribution in Ni-P UBM. Besides, the morphology, mechanical properties of Ni-P-CNT UBM have rarely been reported. In this study, the effects of surfactant dispersant and ultrasonic agitation have been investigated. The microstructure results of mixing CNTs into electroless Ni-

P to form composite Ni-P-CNT coatings were presented. The effects on the shear strength of solder joints by incorporating of a small amount of dispersed CNTs were investigated.

2, Materials and Experiment Procedure

2.1 Materials

Commercial Multiwalled CNTs (grown by chemical vapor deposition with purity ≥ 95%, diameter of about 60 nm and length of 1-2 μm) were provided by ShenZhen Nano Tech. Port Co., Ltd (China). The surfactants polyvinylpyrrolidone (PVP, PVP10-500G,Sigma-Aldrich) and solvent DMAc (99.5%, International Lab USA) were used as-received to fully de-bundle the CNTs. Cu plates (6 mm thick, 99.98 wt.%) were used as substrate for both Ni-P and Ni-P-CNT plating. Commercial acidic sodium hypophosphite bath for electroless plating was obtained from MacDermid, and used with further adjustment.

2.2 Pre-treatment of CNTs and Cu Substrate

Liquid-phase chemical oxidative pre-treatment is employed in this experiment to remove impurities and residues that adhered to CNTs. Firstly, the CNTs were purified with HCl (37 wt. %) under ultrasonic bath (BRANSON B5210E, 47 kHz) for 0.5 hour at room temperature, then the purified CNTs were refluxed in concentrated HNO_3 (67 wt. %) at 70°C for 10 hours. After the above treatments, the CNTs were dispersed in DMAc, which is a water-miscible and high boiling point solvent, with a concentration of 1.0 wt.%. After mixing CNTs into the solvent, all the samples were treated with centrifuge to remove tangles of CNTs and large particles. Then all the samples were kept in an ultrasonic bath for 0.5 hour at room temperature to achieve visibly stable dispersion. Finally, the CNTs were filtered, washed and dried at 80 °C in incubator. Each of the above steps was followed by de-ionized water washing.

As the roughness of Cu substrate is directly related to the brittleness and adhesion ability of the composite coatings, thus prior to the electroless plating, the Cu substrates were polished to micrometer surface finish and etched with HNO_3 (30 vol.%) for 30 s to eliminate scratches and metallic oxide impurities from Cu surface. Then the Cu substrate was immersed in commercial Ru activation solution for surface activation.

2.3 Electroless plating

To deposit smooth Ni-P composite coating surface with uniform CNTs reinforcement, two challenges should be overcome. Firstly, the foreign reinforcement particles, CNTs in this experiment, should be uniformly dispersed in the entire electroless bath and form stable CNTs suspension, neither precipitating nor separating into layers. Secondly, the given plating parameters should be adjusted due to the introducing of CNTs, which will possibly destroy the original balance and stability of the commercial plating bath.

The electroless Ni-P-CNT plating bath was prepared by disperse CNTs into the commercial Ni-P plating solution (from MacDermid). Before electroless plating process, the surfactant PVP was added into the CNT suspension solution. The surfactant dispersant PVP can improve the dispersion by reducing the surface tension and increasing the wettability of CNTs. Then the solution was magnetic stirred at 600 rpm for 10 hours to de-bundle the CNTs clusters by further eliminating the van der Waals force. The Ni-P-CNT plating bath was ultrasonic processed for another 3 hours to avoid agglomeration, and the ultrasonic agitation continued in the entire process. A sample without ultrasonic agitation was also prepared for comparism.

This alkaline Ni-P bath contains nickel sulphate (NiSO4.6H2O) as nickel sources, sodium hypophosphite as a reducing agent along with sodium citrate as the complexion and buffering

agent. The plain Ni-P electroless plating without addition of CNTs was also conducted following the similar procedures.The plating was carried out in a thermal statically controlled bath, and the parameters for both Ni-P-CNT and Ni-P plating are listed in table 1, and the summary of process can be seen in Fig. 1.

Concentration of NiSO4.6H2O	26g/L
Concentration of NaH2PO2.H2O	12g/L
Concentration of Na3C6H5O7.2H2O	75g/L
Concentration of PVP	1×10^{-3}g/L
Concentration of CNTs	1g/L
Plating Temperature	88 ±2°C
Plating pH level	5.3
Plating Time	30 min

Table 1 Bath composition and operating conditions of electroless plating for Ni-P-CNT composite coatings

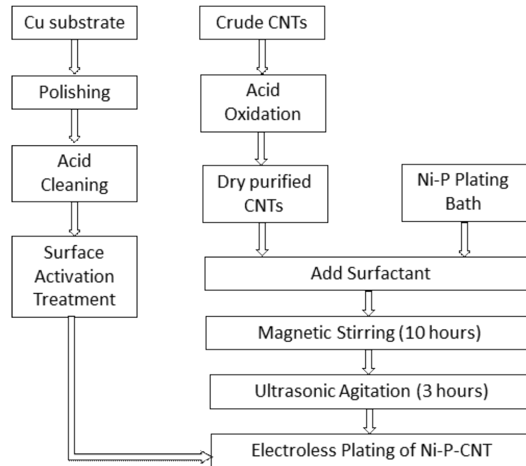

Fig. 1 Flow Chart of the preparation of Ni-P-CNT composites on the Cu substrate

2.4 Morphology and mechanical properties

The surface morphology of the Ni-P-CNT and Ni-P layers was observed by atomic force microscope (AFM, Park Systems) and scanning electron microscope (SEM, JEOL, JSM-7600). CNTs after plating process were observed with Transmission Electron Microscopy (TEM, JEOL, and JEM-2010F). Sn-3.5Ag-0.5Cu solder balls were used to form solder joints with Ni-P-CNT and Ni-P UBM. The soldering process was carried out in an 8-zone forced convection reflow oven (BTU Pyramax 100N, North Billerica, MA). The reflow profile was set with a peak temperature of 250 °C; and the time above the melting temperature of the Sn-3.5Ag-0.5Cu solder was about 70 seconds. Ball shear tests were performed on samples using a shear testing machine (DAGE Series 4000 Bond tester, UK) with a test speed of 350 μm/s. Shear stress testing of 30 solder balls was undertaken at each condition, with the minimum and maximum values removed.

3, Results and Discussion

3.1 Characterization of the pre-treated CNTs

It is well-known that the dispersion of CNTs is the key factor for successful incorporation, because CNTs has strong tendency to agglomerate. There are two reasons for the agglomeration: (1) almost any synthesis approach can hardly guarantee the purity of CNTs product to be 100%. There are always amorphous carbon, fullerene, graphite particles and even metal catalysts adhering to the CNTs. The existence of these impurities will have direct impact on the electroless plating quality. (2) CNTs will aggregate in both electroless bath and deposited coatings, because of the high surface energy and large curvature [20]. These clusters, which can glide easily, will degrade the mechanical strength of CNTs; moreover, the large clusters will result in voids in composite coating. Therefore, the acid oxidation treatment is employed in this study, and the impure carbon particles will be removed after the reaction with acid.

Because the carbon atoms that form CNTs are fixed in a hexagonal, each carbon atom is covalent bonded to three other carbon atoms, which are more chemically stable than amorphous carbon and graphite particles. If the reaction time and processing condition is carefully and accurately controlled, only carbon impurities and residues will be consumed by acid and leave CNTs intact. In this way, the unwanted carbon byproducts, which caused agglomeration, can be removed. Compare Fig.2 (a1) with Fig.2 (a2), after acid oxidation treatment with the environment temperature of 70°C, the serious agglomerates, size of which is about 1-2 μm, have been fully eliminated. No large agglomerates can be observed in the CNTs sample after 10 hours of acid treatment. Meanwhile, the curvature and the aggregation level between single CNT has been reduced effectively.

It can be seen from the Fig.2 (b1), an irregular long CNT intertwined with other CNTs, and therefore a strong oxidative HNO_3 treatment was employed in this experiment to shorten long CNTs. The results after the acid treatment was shown in Fig.2 (b2), no obvious long and thick CNTs existed in the sample. It is because the crude CNTs are capped on both ends by half-spherical fullerene fragments, which is not in hexagonal structure, so the fullerene will be peeled off after the acid reaction. Then the acid filled in the hollow space of the CNTs, and reacted with its inner walls. After the inner wall become thinner, the long and thick CNTs will be cut into shorter tubes, and in this way the length and diameter of CNTs are more uniform after the acid treatment. Normally, short CNT fibers have less tendency of agglomeration, so better dispersion can be achieved by making the length smaller.

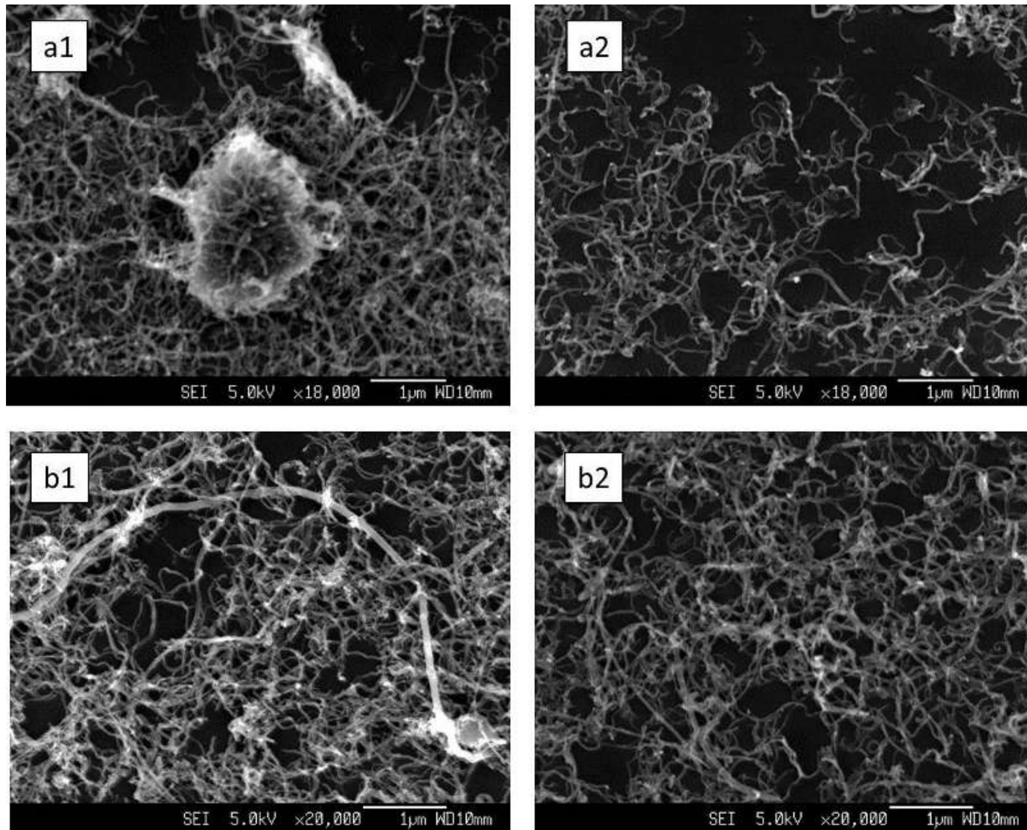

Fig. 2 SEM micrographs of (a1)(b1) CNTs before acid treatment (a2)(b2) CNTs after acid treatment

3.2 Effects of surfactant and ultrasonic agitation

Even though the tendency of forming large agglomerates has decreased effectively after acid treatment, and the length has become more uniform, the tangle phenomenon still exist between individual CNT. Therefore, surfactant and ultrasonic agitation were introduced to disperse these nano-scaled CNT fibers in electroless plating bath. Both surfactant and ultrasonic agitation can accelerate the breakup of the agglomerated CNTs, which was necessary to obtain homogeneous Ni-P-CNT composite coatings.

It is well know that van der Waals force made the CNTs aggregate into clusters, so adding surfactant is an effective approach to de-bundle them. The surfactant used in this experiment is PVP. The molecular chain of PVP surrounded and adhered to the outer walls of CNTs, which enhanced the wettability of CNTs [21,22]. At the same time, stability of suspension and the electrostatic adsorption of suspended CNTs on substrate can be improved by coating CNTs with PVP surfactant dispersant.

The surface morphology of Ni-P-CNT composite coatings without ultrasonic agitation is shown in Fig.3 (a). The surface of the Ni-P-CNT composite coatings were covered by irregular shaped particles, with the average size of 1-2 μm, and the surface was not smooth because of these uneven bumpy nodules. It is because metal atoms can hardly cover CNT agglomerations continuously, they can only cover CNT agglomerations as isolated particles, which made the surface unsmooth and uncontinuous.

The surface morphology of Ni-P-CNT composite coatings with surfactant and ultrasonic agitation is shown in Fig.3 (b). The surface was compact and exhibited a nodular shape with a typical cauliflower-like morphology. There were no irregular shaped particles and bumpy nodules on the surface and the CNTs were evenly distributed and embedded in the coating matrix.

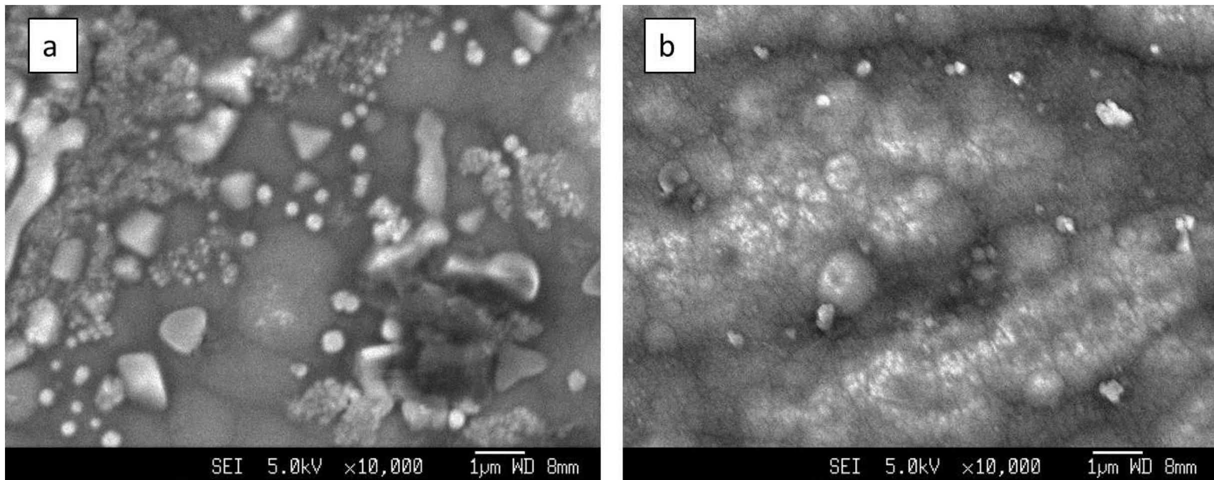

Fig. 3 SEM micrographs of Ni-P-CNT composite coatings (a) without surfactant and ultrasonic agitation (b) with surfactant and ultrasonic agitation

Before understanding the effects of ultrasonic agitation, it is necessary to explore the deposition mechanism of composite deposition of CNTs with Nickel. There are two plating mechanisms proposed: the first mechanism suggested that, before adhering to Cu substrate, each individual CNT was covered by Ni particles first and gradually full coated. The first stage of the plating is to form Ni-coated CNTs, while the second stage is to co-deposit Ni-P and Ni-coated CNT composite coatings on substrate. The other suggested that, the pristine CNT was adsorbed to substrate first, and the plating reaction take place simultaneously on both substrate and adsorbed CNTs. Fig.4 shows the micrograph of a recycled CNT sediment after electroless plating conducted at 88 ℃ for 30 mins. It can be observed the dark spots are Ni particles deposited from the plating bath, and less than 10 Ni particles exited on the outer wall of a CNTs. The TEM results support the second mechanism better that co-deposition process take place on CNTs and substrate simultaneously.

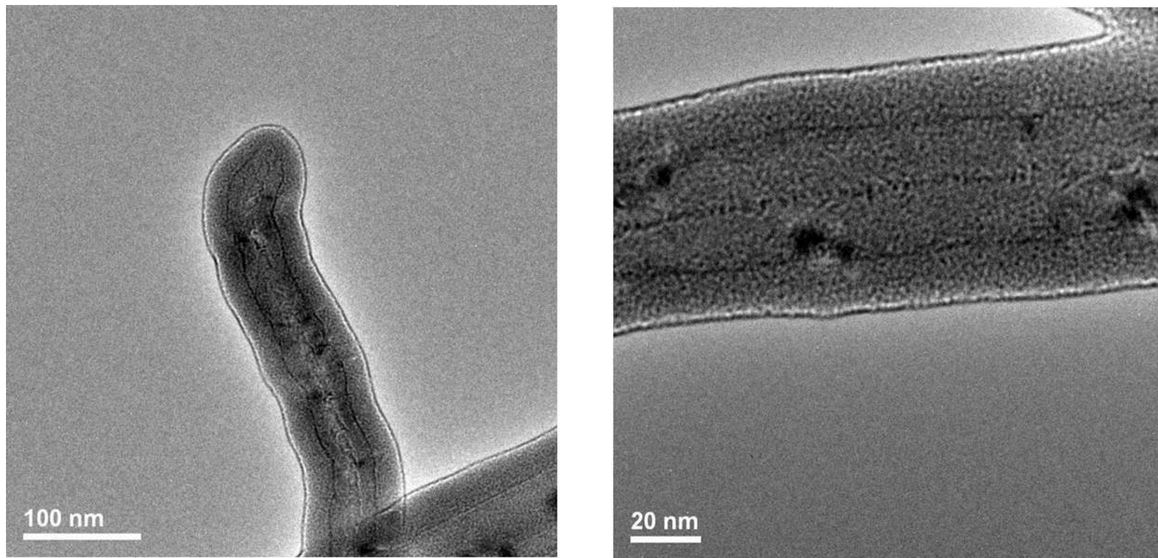

Fig. 4 TEM image of a recycled CNT residue with electroless plating conducted at 88 ◦C for 30 min

According to second mechanism, it can be assumed that the composite deposition of CNTs and Ni-P includes four stages: (1) Homogeneous and stable suspension plating bath is maintained; (2) The CNTs moved towards the substrate by diffusion; (3) Weak adsorption between CNTs and substrate was formed; (4) CNTs were wrapped and covered by Ni particles, and embedded in Ni matrix along with the deposition process. The composite plating process with ultrasonic agitation was illustrated in Fig.5. Firstly, the CNTs moved towards the substrate by diffusing force, along with the ultrasonic wave, agglomeration were prevented. Ultrasonic wave can drive more CNTs move towards substrate, which can expedite the co-deposition speed. Secondly, CNTs arrived at the substrate surface and a weak adsorption was formed between them. And the CNTs which do not have direct contact with the substrate were shaken and driven away. Then, the Ni particles began to deposit on the surface of the substrate and covered the CNTs simultaneously. Finally, all the CNTs were embedded in the Ni matrix, and strong bonds between CNTs and deposited layers were formed. It can be concluded that, ultrasonic agitation is

beneficial to plating process by reducing agglomerates, which made the deposited layer smoother and the distribution is more uniform.

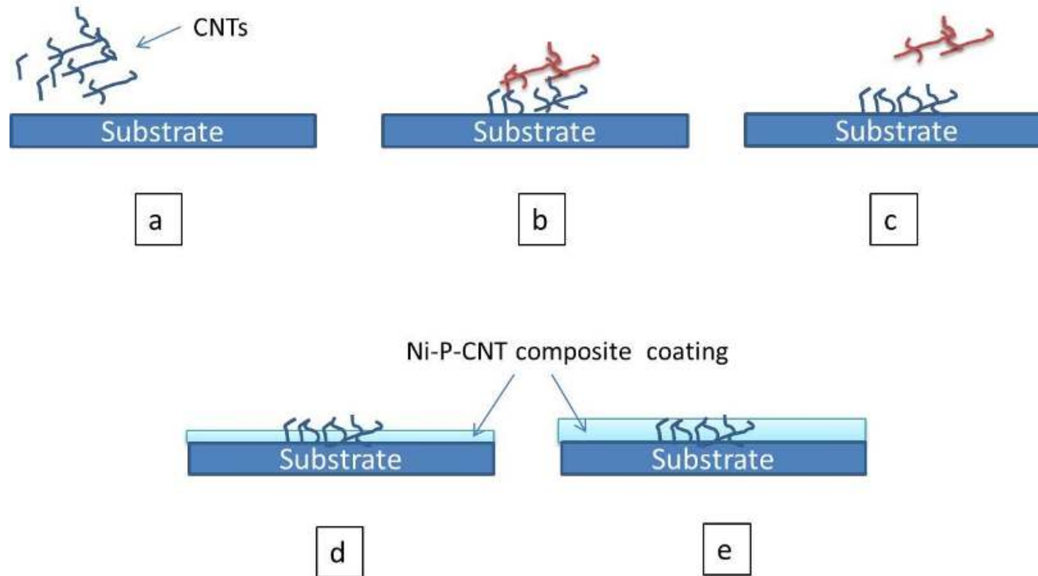

Fig. 5 composite Ni-P-CNT coating process by electroless plating with ultrasonic agitation

3.3 Microstructure of Ni-P-CNT composite coatings

According to the report of LY Wang, the volume fraction of CNTs in the composite coatings were calculated to be 5.1 vol. %, when the CNT content in the bath was 1g/L [23]. It is very important, as the volume fraction of CNTs in the coatings doesn't increase linearly with the CNT content in bath.

Fig.6 (a) is a SEM micrograph of Ni-P-CNT composite coatings. The surface was compact and continuous, shown a typical cauliflower-like morphology, with CNTs uniformly dispersed in it. At the same time, the CNTs were embedded in the metal matrix, no pores and clusters were present, which is very beneficial for conductivity, corrosion resistance and mechanical strength. The compact and continuous surface should attributes to the well dispersion of CNTs, which is

the key factor for homogeneous CNT distribution. If the CNTs aggregated as clusters, the metal atoms can only deposit on the outer layer of CNT clusters, and the inner layer of CNT clusters will glide away, which resulted in voids or holes. In Fig 6(b) is a SEM micrograph of an individual embedded CNT. The CNT was not presented in agglomeration morphology, instead it was deeply contacted with the metal matrix and no voids existed around the CNT. This proved that metal atoms can continuously deposit on individual CNTs, which is beneficial to form void-free surface. It can also be observed that the diameter of CNTs have slightly increased, because some of the CNTs were wrapped and covered by Ni particles during the plating process. This is very advantageous in forming bonds between CNTs and Ni matrix.

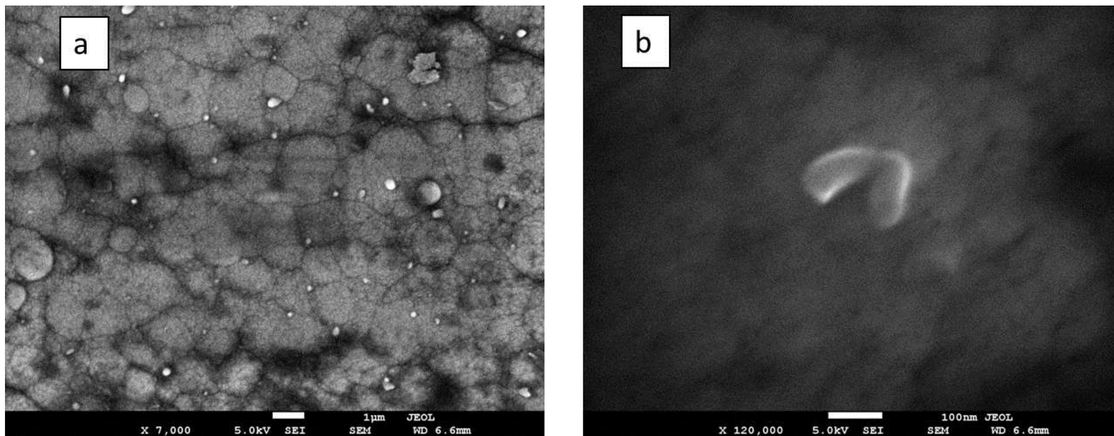

Fig. 6 Surface morphology of Ni-P-CNT composite coatings (a)low magnification (b)high magnification

The electrolessly deposited Ni-P and Ni-P-CNT composite coatings were shown in Fig.7. It can be observed that uniform and continuous coatings were formed and the surfaces of both sample were uniformly covered. As shown in Fig. 7 (a), the surface of plain Ni-P coatings were smooth and exhibited a nodular shape with the average size of 2 μm, and there were no obvious

protuberance can be seen. However, it is very obvious that several micro voids appeared between the nodule edges. It is because the micro bubbles that formed during the plating reaction, inappropriately adhered to the surface of deposited layer, which made the coating porous in the end. These micro voids are highly disadvantageous to the corrosion resistance, mechanical strength as well as conductivity of composite coatings. Fig. 7 (b) has shown the surface morphology of Ni-P-CNT composite coatings for comparison. The CNTs were uniformly distributed in the electrolessly deposited film, and they were well bonded and embedded in the metal matrix. Compared to the plain Ni-P coatings, no micro voids can be seen in the entire area, which ensures better corrosion resistance and the nodule size of Ni-P-CNT was smaller. The small nodule size reveals higher reaction rate in the process. CNTs, which have large curvature and surface energy, expedited the reaction rate nearby by providing more active reaction area. Therefore, due to the existence of CNTs, the particle and deposited nodule size is much finer in the Ni-P-CNTs composite coatings. In the red circle of Fig.7 (b) was a protuberance on the composite coatings, which was resulted from CNT clusters that acted as impurity center during the electroless plating.

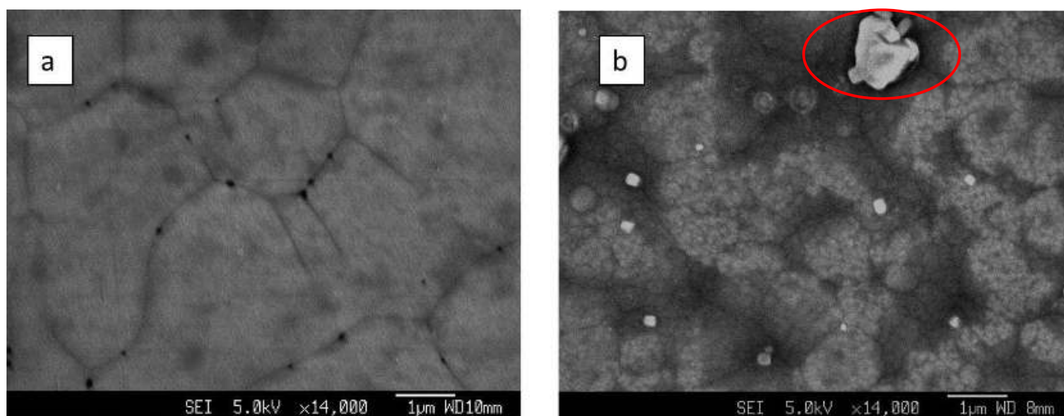

Fig. 7 microstructure of (a)Ni-P composite coatings (b)Ni-P-CNT composite coatings

The AFM images of the surface topography of both Ni-P and Ni-P-CNT composite coatings were studied, the scanning area is 5μm ×5μm. In Fig. 8 (a), The topographic image of plain Ni-P coating showed a variation in height, the root mean square roughness of the plain Ni-P coating was 68 nm, with a peak to peak roughness of 295 nm. The surface cross-section analysis was marked with red line in the image, which showed distribution of hills and valleys. As observed from the line profile, the size of hills and valleys were around 1 μm, and the height difference was around 100 nm. This was in accordance with Fig 8(a) that micro voids were formed between the nodule edges, which made the surface unsmooth and porous. On the other hand, the root mean square roughness of Ni-P-CNT composite coatings was 24 nm, and the peak to peak roughness was 121 nm. The surface cross-section analysis of Ni-P-CNT exhibited a more uniform and finer distribution of hills and valleys as compared to plain Ni-P coatings. The size of hills and valleys were around 0.5 μm, and the height difference is around 50 nm. The decreased roughness indicated that the surface of Ni-P-CNT coatings was much smoother than plain Ni-P coatings, which is because the CNTs filled the micro voids in metal matrix.

Based on the SEM and AFM images above, it can be proved that the as-prepared Ni-P-CNT composite coatings have shown a more uniform, continuous and compact surface morphology than the plain Ni-P coatings.

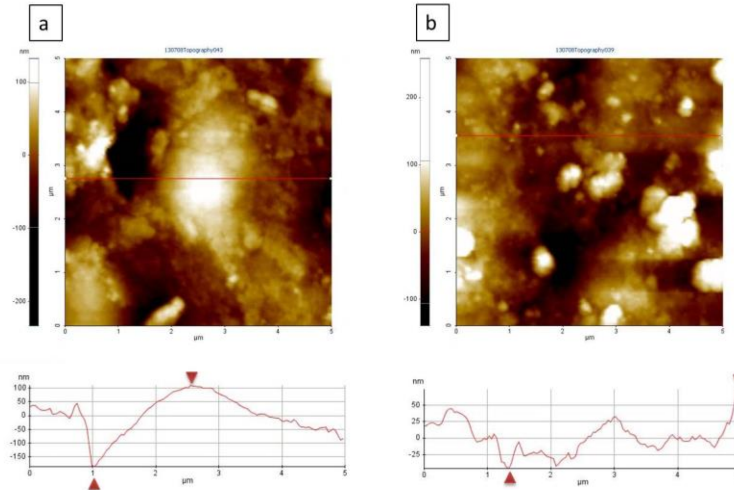

Fig. 8 AFM image of the topography of (a)Ni-P composite coatings (b)Ni-P-CNT composite coatings

3.4 Shear strength of Ni-P-CNT composite coatings

The joints formed between pad and solder, not only provide electrical path between components, but also subjected to mechanical loadings. In order to mimic the real service conditions used in microelectronic industry, the shear test was an essential mechanical property regarding the reliability. Shear tests were conducted in this study to evaluate the effect of CNT reinforcement on the mechanical properties of joints as a function of reflow cycles.

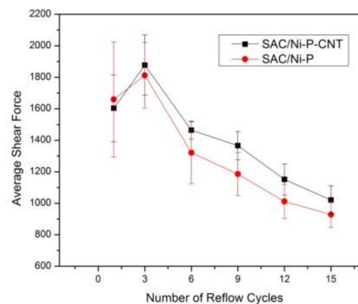

Fig. 9 Average shear strength of solder joints as a function of number of reflow cycles

Fig. 9 plotted the variation of shear strength of the solder joints on both coatings as a function of number of reflow cycles. For both kinds of coatings, the shear strength increased at first and decreased monotonically after 3 reflow cycles, which was in accordance with published results. The average shearing force of Sn-3.5Ag-0.25Cu solder/Ni-P-CNT is generally bigger than that of the Sn-3.5Ag-0.25Cu solder/Ni-P joints after 6 reflow cycles. The variation in behavior is controlled by several factors.

On the one hand, repeated reflow cycles can enlarge the contact area of both Sn-3.5Ag-0.25Cu solder/Ni–P and Sn-3.5Ag-0.25Cu solder/Ni–P-CNT joints. And intermetallic compound (IMC) will be formed after reflow cycles, which will strengthen the joints between pad and solder. For the solder joints with CNT addition, the CNT fiber can also enhance the bond strength after several reflow cycles. On the other hand, excessively repeated heating and cooling process of reflow would degrade the solder joints due to microstructural phase coarsening, thermal stress concentrations and volumetric shrinkage of the solder joints. Thus, the strength of the solder joints would be weakened after multiple reflows. Nevertheless, even though both coatings were weakened after multiple reflows, the Ni-P-CNT coating demonstrated better mechanical properties. It is well known, like mechanical strength of clay was reinforced by grass straw, the solder joints can be strengthen by adding reinforcing fibers to the metal matrix. However, the mechanical properties of reinforcement phase are key to the mechanical strength of the entire joints. If the reinforcement phase is too stiff, and without elasticity, then this phase will have high possibility to crack first; If the reinforcement phase is too weak, the stress cannot be transfer from the matrix material to the reinforcement phase. Therefore, CNTs act as a perfect reinforcement phase due to its high elasticity. The shear stress was transferred from matrix materials to CNTs, and some of the breaking force was absorbed by CNTs when the solder was

torn apart from the pad. Fig.10 showed a cross-section SEM image of a torn pad, one end of the CNT were protruding from the surface with another end embedded in metal matrix. Thus, the CNTs and metal not only have mutual physical adhesion, but also have some interfacial bonds.

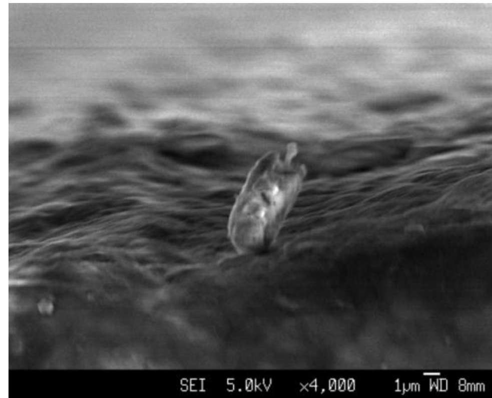

Fig. 10 Cross-section SEM image of a torn pad: showing the CNT embedded in the pad coating

3.5 Factors affecting plating process

Composite Ni-P-CNT plating is more complicated than plain Ni-P plating, several factors will affect the quality of deposited layers. Therefore, the plating conditions should be optimized before conducting plating process.

Firstly, the elevated pH level will accelerate the depositing speed. However if the pH level is too high, the plating solution is easy to decompose, and the deposited layer will be porous and incompact. The optimum pH level was adjusted 5.3 in this study.

Secondly, the magnetic stirring speed also affects the plating quality. If the magnetic stirring speed is less than 200 rpm and the stirring time is less than 3 hours, the CNTs cannot disperse in the solution. If the striking speed is higher than 800 rpm, the plating solution is unstable and easy

to decompose. Thus, the magnetic stirring speed used in this study was 600 rpm, which enabled CNTs to wet, de-bundle and stabilize.

Thirdly, the CNT concentration in the plating bath has direct effect on the CNT content in the composite coatings. The CNT content in the Ni-P-CNT coatings increased with the CNT concentration in the plating bath at the early stage, due to the higher contact rate and adhesion rate. After a certain “saturation value”, the CNTs are difficult to disperse in the plating bath, which will lead to agglomerations. Meanwhile, if the CNT concentration is too high, the CNTs will become active nucleation site itself, and the Ni particles tend to deposit on CNTs rather than Cu substrate. Thus, it is recommended the CNT concentration should be lower than 2g/L in plating bath.

Fourthly, the plating temperature is another key parameter affecting plating process. The deposit rate is very low under 80°C, because both diffusion and activity is very limited under that temperature. If the temperature is higher than 95°C, the plating bath will become very unstable and easy to decompose. So the optimum plating temperature should be 88 ±2°C in this study.

4, Conclusions

In order to disperse carbon nanotubes in electroless Ni-P coatings, different approaches were employed in this study. Acid oxidation is a covalent chemical modification method which can cut long and thick CTNs into short fragments. Appropriate amount of surfactant addition can significantly improve the dispersion wrapping individual CNT with molecular chains. Magnetic stirring and ultrasonic agitation are non-destructive dispersion method. Magnetic stirring can help de-bundle large clusters while ultrasonic agitation can accelerate the breakup of CNT agglomerations and let CNTs homogeneously distributed on the deposited coatings. It was

verified that the dispersion can be significantly improved after proper treatment process, and surface of the coating layer is quite smooth; CNTs are equably dispersed throughout the matrix. In addition, the interfacial bonding between CNTs and Ni-P alloy is good. Shear tests were conducted to evaluate the effect of CNT reinforcement on the mechanical properties of joints. For the solder joints with CNT addition, the CNT fiber can also enhance the bond strength after several reflow cycles. Even though the strength of the solder joints would be weakened after multiple reflows, the Ni-P-CNT coating still demonstrated better mechanical properties by transferring mechanical loadings. Moreover, deposition mechanism of CNTs with Ni was analyzed. The composite deposition of CNTs and Ni-P includes four stages: (1) Homogeneous and stable suspension plating bath is maintained; (2) The CNTs moved towards the substrate by diffusion; (3) Weak adsorption between CNTs and substrate was formed; (4) CNTs were wrapped and covered by Ni particles, and embedded in Ni matrix along with the deposition process. Factors that affecting plating process was also discussed, and the plating condition was suggested as following: Optimum pH level was 5.3; optimum magnetic stirring speed was 600 rpm; recommended the CNT concentration should be lower than 2g/L in plating bath; and optimum plating temperature was 88 ±2°C.

Acknowledgments

The authors would like to acknowledge the financial support provided by the Research Grants Council, Hong Kong, Ref. No. 9041636 (A study of nanostructured electronic interconnects-preparation, characterization and integration), City University of Hong Kong Research project: 7002848 (A study of functionalized CNT/graphene reinforced composite electronic interconnects: preparation, characterization and integration for green nanoelectronic applications”.

Reference

1. Y. C. Chan, D. Yang, Prog. Mater. Sci. **55**, 428-475 (2010)

2. L. Hua, Y.C. Chan, Y.P. Wu, B.Y. Wu, J. Hazard. Mater. **163**, 1360-1368 (2009)

3. D. Yang, Y. C. Chan, K. N. Tu, Appl. Phys. Lett. **93**, 041907 (2008).

4. M.O. Alam, H. Lu, C. Bailey, and Y.C. Chan, Comp. Mater. Sci. **45**, 576-583(2009)

5. J. Shen and Y.C. Chan, Microelectron. Reliab. **49**, 223–234 (2009)

6. F. Gao, J.P. Lucas, K.N. Subramanian, J. Mater. Sci. Mater. Electron. **12**, 27–35 (2001)

7. F. Gao, J. Lee, S. Choi, J.P. Lucas, T.R. Bieler, K.N. Subramanian, J. Electron. Mater. **30**, 1073–1082. (2001)

8. J. Shen, Y. Liu, D. Wang, H. Gao, J. Mater. Sci. Technol. **22**, 529–532 (2006)

9. A. K. Gain, Y.C. Chan, Winco K.C. Yung Microelectron. Reliab. **51**, 975–984 (2011).

10. C.F.Tseng, C.J.Lee, J.G.Duh, Mater.Sci.Eng.A – Struct.Mater.Prop.Microstruct. Process. **574**, 60–67 (2013)

11. C.F.Tseng,J.G.Duh,Mater.Sci.Eng.A – Struct.Mater.Prop.Microstruct.Process. **580**, 169–174 (2013).

12. K. Hari Krishnan, S. John, K. N. Srinivasan, J. Praveen, M. Ganesan, P. M. Kavimani, Metall. Mater. Trans. A, **37**, 1917-1926 (2006)

13. R. C. Agarwala, Vijaya Agarwala, Sadhana , **28**, 475-493(2003)

14. S. Iijima, Nature, **354**, 56-58 (1991)

15. T. W. Ebbesen, H. J. Lezec, H. Hiura, J. W. Bennett, H. F. Ghaemi, T. Thio, Nature, **382**, 54-56 (1996)

16. P. Kim, L. Shi, A. Majumdar, P. L. McEuen, Phys. Rev. Lett. **87**, 5502 (2001)

17. M. F. Yu, Bradley S. Files, S.Arepalli, Rodney S. Ruoff, Phys. Rev. Lett. **84**, 5552-5555 (2000).

18. Z. Yang, H. Xu, Y.L. Shi, M.K. Li, Y. Huang, H.L. Li, Mater. Res. Bull. **40** (2005) 1001–1009

19. A. Zarebidaki, SR.Allahkaram, J Alloy Compd. **509**, 1836–1840 (2011)

20. Sie Chin Tjong, Carbon nanotube reinforced composites : metal and ceramic matrices, (Wiley, New York, 2009)

21. L. Vaisman, H. Daniel Wagner, G. Marom, Adv. Colloid Interfac. **128–130**, 37–46 (2006)

22. Q. Y. Tang, I. Shafiq, Y. C. Chan, N. B. Wong, and R. Cheung, J. Nanosci. Nanotechno. **10**, 4967–4974 (2010)

23. L.Y. Wang, J.P. Tu, , W.X. Chen, Y.C. Wang, X.K. Liu, Charls Olk, D.H. Cheng, X.B. Zhang, Wear, **254**, 1289–1293 (2003)